ACS OMEGA

http://pubs.acs.org/journal/acsodf

Article

Bulky Di(1-adamantyl)phosphinous Acid-Ligated Pd(II) Precatalysts for Suzuki Reactions of Unreactive Aryl Chlorides

He-Xin Xiao, Wan-Yun Hsu, Siou-Wei Liang, Yingjie Guo, Wan-Ching Lee, I-Chung Lu, and Yu-Chang Chang*

Cite This: *ACS Omega* 2021, 6, 35134–35143

Read Online

ACCESS | Metrics & More | Article Recommendations | Supporting Information

ABSTRACT: Di(1-adamantyl)phosphine oxide (SPO-Ad: Ad_2P-(V)(=O)H), a stable tautomer of di(1-adamantyl)phosphinous acid (PA-Ad: Ad_2P(III)-OH), was employed to synthesize two new PA-Ad-coordinated complexes, POPd-Ad and POPd2-Ad. POPd-Ad was easily transformed from POPd2-Ad in acetonitrile, and the $[M - H]^-$ ion of the deprotonated POPd-Ad was observed in the electrospray ionization-mass spectrum of POPd2-Ad. Both complexes are effective precatalysts for the Suzuki reaction of aryl chlorides. The reduction of Pd(II) in POPd-Ad and POPd2-Ad by arylboronic acid was examined, and the ideal Pd-to-PA ratio in the Suzuki reaction was found to be 1:1. The effect of temperature on the catalytic yields was studied to examine the possible ligation state of the active species and the dimer-to-monomer process of POPd2-Ad. Mononuclear and mono-ligated Pd species was assumed to be catalytically active. The electronic and steric effects of PA-Ad were slightly better than those reported for PA-tBu ($^tBu_2P$(III)-OH). Density functional theory calculations were performed to evaluate the formation of mono-ligated and mononuclear Pd species from POPd-Ad and POPd2-Ad. Furthermore, the reaction time and catalyst loading could be reduced for the reported POPd1-tBu precatalyst using the optimized reaction conditions for POPd-Ad. The complexes synthesized in this extensive study will complement the existing SPO-coordinated POPd series of precatalysts.

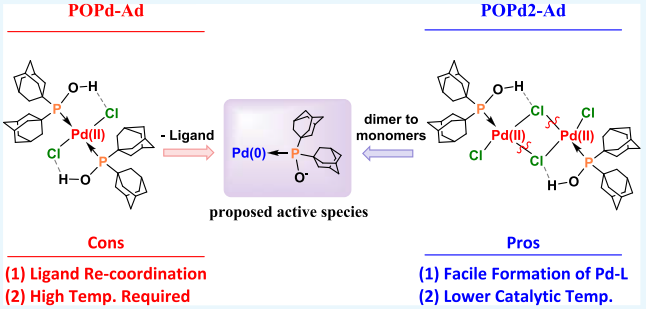

INTRODUCTION

Transition-metal (TM)-catalyzed cross-coupling reactions have been extensively researched because of their broad application areas such as in the synthesis of natural products[1] and in materials science.[2] Moreover, TM-catalyzed decarbonylative coupling of acyl fluorides[3] and N-acyl-amides,[4] as well as TM-catalyzed acylative[5] cross-coupling reactions have been extensively studied.[6] The successful advancements in these reactions are highly correlated to the continual progress of TM catalysts.[7] Auxiliary ligands, in particular, play a central role in the development of new TM catalysts.[8] For instance, phosphines,[9] N-heterocyclic carbenes (NHC),[10] and carbodicarbenes,[11] have been proven effective ligands for Pd-catalyzed cross-coupling reactions.

The phosphinous acid ligand (PA-R: R_2P(III)-OH, with -R being the substitutions on PA) is a promising analogue of trisubstituted phosphines (PR_3) (Scheme 1).[12] PA-R can be easily tautomerized from the secondary phosphine oxide (SPO-R: R_2P(V)(=O)H) in the presence of TM complexes (Scheme 1).[13] Li et al. previously showed that di-tert-butyl phosphine oxide (SPO-tBu: $^tBu_2P$(=O)H) and its related Pd(II) complexes are effective preligands and precatalysts for various Pd(II)-catalyzed cross-coupling reactions.[14] Considering the stoichiometry and the bulkiness of substituents on

Scheme 1. Tautomerization of SPO-R to PA-R and Syntheses of Prototype PA-Coordinated Pd(II) Complexes

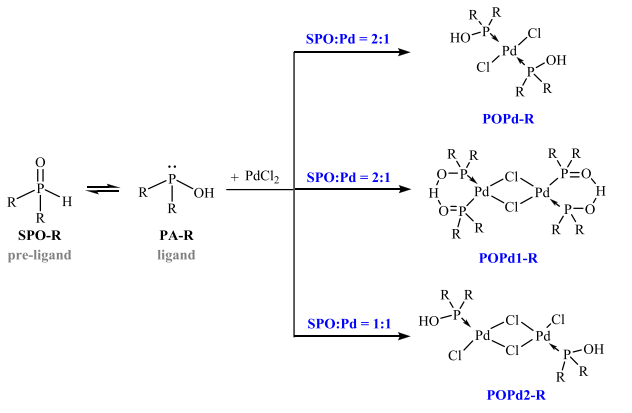

Received: November 15, 2021
Accepted: November 25, 2021
Published: December 8, 2021

https://doi.org/10.1021/acsomega.1c06430
ACS Omega 2021, 6, 35134–35143

SPO-R, three types of Pd(II) complexes can be obtained (Scheme 1).[14b,c] According to the literature as well as from reported experiments, SPO-R equipped with bulky substituents tends to form POPd-R and POPd2-R,[14a] while SPO-R functionalized with less bulky groups yields POPd-R and POPd1-R.[15] Similar observations were reported when sterically different SPO-R preligands were reacted with $PtCl_2(COD)$.[13a] Notably, PA-R has rich coordination modes, as reported in the literature.[16]

The steric effect of the two substituents on the coordinated PA-R has a noticeable impact on the catalytic capability of the associated Pd(II) precatalysts. For example, using aryl chloride as a substrate in the Suzuki reaction, PA-Ph-coordinated POPd1-Ph was reported as an inefficient precatalyst,[17] while the PA-tBu-coordinated POPd1-tBu was demonstrated to be a good precatalyst.[14c] Employing large sterically hindered SPO-R as a preligand, could therefore be considered a promising route to improve catalytic capability.[18] This was shown through the successful employment of secondary phosphine oxides with bulky substituents as preligands in several TM-catalyzed reactions.[19]

Sterically congested PA-Ad coordinated Complex 1 was demonstrated to be an effective precatalyst for the C−H bond arylation of oxazo(*li*)nes (Figure 1a).[20] Moreover, PA-diam

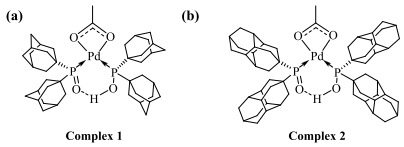

Figure 1. (a) PA-Ad and (b) PA-diam-ligated Pd(II) complexes.

coordinated Complex 2 was reported as a good precatalyst in the Kumada-Corriu cross-coupling reaction of 2-pyridyl Grignard reagents (Figure 1b).[19g] In addition, both complexes are suitable precatalysts for heteroarylation via the C−H activation step.[19i] Ackermann demonstrated that PA-Ad is an efficient ligand in Ru-catalyzed C−H bond functionalization,[21] Ni-catalyzed Kumada cross-coupling reactions,[22] and Pd-catalyzed intramolecular α-arylation reactions.[19f] Crystal structures for these two precatalysts were resolved.[19g,i] Based on the literature, the SPO-Ad preligand has not been used to synthesize the POPd series of complexes. This gap in research might be due to the multiple steps required to synthesize SPO-Ad or the cost associated with SPO-Ad and its precursor di-1-adamantylphosphine chloride.

The percent buried volume ($\%V_{bur}$) parameter[23,24] has been employed to evaluate the steric effect associated with PA-R.[25a,18,25b] Examples where this parameter were successfully employed in the evaluation of the steric effect include the Au ← $P(OH)R_2$ series of complexes where $\%V_{bur}$ parameters of 27.3% for $P(OH)Ph_2$ and 32.6% for $P(OH)^tBu_2$ were reported.[25a] The $\%V_{bur}$ has also been employed in the evaluation of steric effects associated with PR_3 and NHC ligands.[26] For Pd ← PR_3 complexes, the $\%V_{bur}$ parameters for PAd_3 and P^tBu_3 were estimated to be 40.5 and 40.0%, respectively.[27] Therefore, it was expected that Ad_2P-OH and $^tBu_2P$-OH would have comparable steric effects relative to the TM center.

To expand upon the POPd series of precatalysts as reported in the literature, it would therefore be reasonable to synthesize a POPd series of complexes employing a SPO-Ad preligand. Herein, we report the syntheses and crystal structures of such SPO-Ad-coordinated POPd-Ad and POPd2-Ad complexes. POPd2-Ad can be quickly converted to POPd-Ad in acetonitrile at room temperature. These two complexes are shown to be efficient precatalysts for the Suzuki reaction of aryl chlorides. The reduction of Pd(II) in POPd-Ad and POPd2-Ad, the Pd-to-ligand ratio in the catalytic cycle, the ligation state of potential catalytic species, and the possible reaction mechanism are suggested. Based on experimental and density functional theory (DFT) investigations, the formation of monoligated and mononuclear Pd(II) intermediates will be proposed.

RESULTS AND DISCUSSION

Syntheses and Characterization of POPd-Ad and POPd2-Ad. Precatalyst POPd-Ad was synthesized through the reaction of $PdCl_2$ and 2 equiv of SPO-Ad in a nitrogen-gas-filled Schlenk tube at 60 °C for 18 h (Scheme 2a). Because of

Scheme 2. Syntheses of POPd-Ad and POPd2-Ad

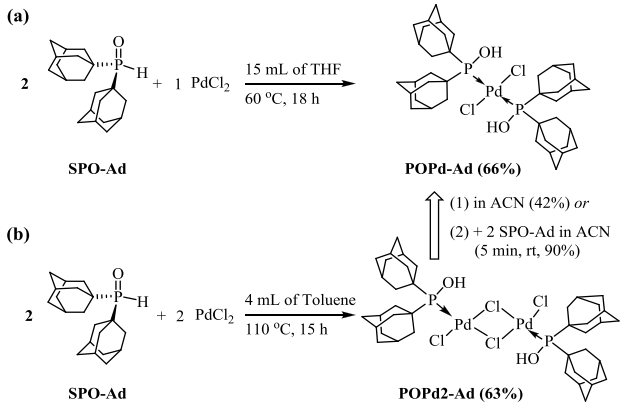

the large steric hindrance associated with SPO-Ad, POPd1-Ad was not produced. Upon decreasing the amount of SPO-Ad to one equivalent and increasing the temperature to 110 °C for 15 h, POPd2-Ad was formed, which precipitated as the main product (Scheme 2b). Following workup and recrystallization processes, the yellow and orange solids produced were characterized as POPd-Ad and POPd2-Ad, respectively. The ^{31}P NMR chemical shifts for POPd-Ad and POPd2-Ad were observed at 113 and 137 ppm, respectively. Additional supporting evidence include the DEPT-90, DEPT-135, and the full one-dimensional (1D) ^{13}C NMR spectra for POPd-Ad and POPd2-Ad, as shown in Figure S1.

Employing a slow evaporation method under ambient conditions, crystals of POPd-Ad (Figure 2) and POPd2-Ad (Table S1) were grown in CH_2Cl_2 for X-ray crystal structure analysis. The molecular structure of POPd-Ad indicates that Pd−P and Pd−Cl bond lengths are 2.3483(5) and 2.3082(6) Å, respectively. The two Pd−P bonds in POPd-Ad are longer than the average bond distance (2.2498 Å) associated with 50 Pd(II)−$P(OH)R_2$ bonds[28] and are among the longest Pd(II) ← $P(OH)R_2$ dative bond distances. This indicated a large steric repulsion between the two adjacent adamantyl substituents on the two Ad_2P-OH ligands. In addition, the two different bond angles of Cl−Pd−P1 are 91.90(2) and 88.09(2)°, while those of P−Pd−P and Cl−Pd−Cl are exactly 180°. The distance between P−OH···Cl indicates the presence of two intramolecular hydrogen bonds (2.272 Å). It could

https://doi.org/10.1021/acsomega.1c06430
ACS Omega 2021, 6, 35134−35143

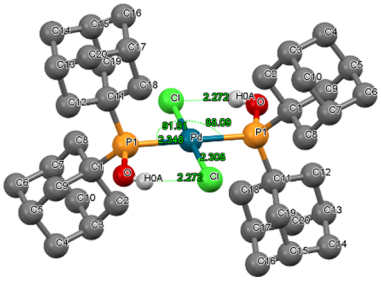

Figure 2. Molecular structure of POPd-Ad. Some hydrogen atoms are omitted for clarity.

therefore be concluded that the POPd-Ad with a d^8 Pd(II) center exhibited a typical square-planar geometry. Although the formation of POPd2-Ad could be confirmed through characterization, the resolution of its X-ray structure was unsatisfactory, with an associated high R-value of 0.2081. Subsequent attempts to grow suitable POPd2-Ad crystals for confirmatory X-ray structure analysis were unsuccessful (Table S1). However, the X-ray structure of POPd2-Ad shows that the Pd_2Cl_2 core is butterfly-shaped, while each Pd center possesses a typical square-planar geometry.

Although POPd2-Ad spontaneously dissociated to form POPd-Ad in acetonitrile (Method (1) in Scheme 2: 42%), this phenomenon was not observed in toluene, tetrahydrofuran (THF), or 1,4-dioxane (Table S2). Reacting POPd2-Ad with 2 equiv of SPO-Ad in acetonitrile for 5 min at room temperature resulted in a high yield of POPd-Ad (Method (2) in Scheme 2; 90%). During the evaluation of electrospray ionization (ESI)-mass spectra of these products (Figures 3 and S2), $[M - H]^-$ ions identified at m/z 813.33 and m/z 990.51 could be attributed to POPd-Ad and POPd2-Ad, respectively. In addition, $[M - H]^-$ ions at m/z 813.33 associated with POPd-Ad were also detected in the mass spectrum of POPd2-Ad. Several additional species detected in the mass spectrum of POPd2-Ad are presented in Figure 3. A comparison between the theoretical and observed isotope patterns was subsequently performed to validate the predicted structures. Here, ion species B, C, E, G, H, and I could be generated from the $[M - H]^-$ ion of POPd2-Ad, through dimer-to-monomer dissociation (B, C) or the dissociation of PA-Ad (E) or Cl^- (G). Species H could be formed from the association of $PdCl_2$ with G (Figure 3b), while species I could be generated from the recombination of D and G (Figure 3b). Attempts to predict the minor anionic species observed at m/z 631.08 were not successful. The observed $[M - H]^-$ ion of POPd-Ad was attributed to the combination of species B and F (PA-Ad). The B ($PdCl_2$ ← $P(O^-)Ad_2$), C, and I were the three most abundant ionic species (Figure S2a).

Assessment of the Electronic and Steric Effects of PA Ligands. Previously,[29] $R_2(HO)P \rightarrow Ni(CO)_3$ was used to evaluate the electron-donating ability ($\nu\sim_{CO}$, A1 stretching mode) of PA-R. For nickel model complexes, the reported extrapolated Tolman electronic parameters (TEP, $\nu\sim_{CO}$*0.9540) for $^t Bu_2(HO)P$ and $Ad_2(HO)P$ were 2064 and 2061 cm^{-1}, respectively. This result indicates that $Ad_2(HO)P$ is more efficient in donating electron density to the TM center as compared to $^t Bu_2(HO)P$. Extrapolated TEPs of 2010 and 2009 cm^{-1} were also reported for $^t Bu_2P\text{-}O^-$ and $Ad_2P\text{-}O^-$ sets, respectively.[29] Because salt is present in many cross-coupling reactions, $R_2(HO)P$ may have deprotonated and interacted with cations in catalytic reactions. Based on this

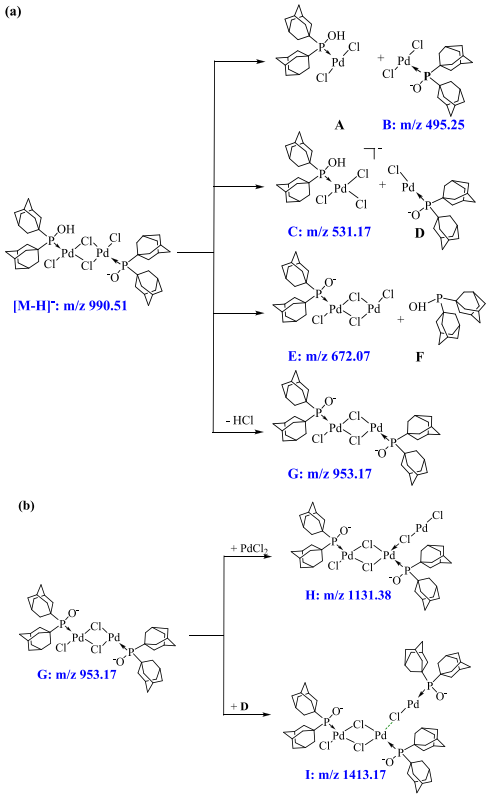

Figure 3. Negatively charged species (a) **B**, **C**, **E**, **G**, and (**b**) **H**, **I** detected using the ESI mass spectrometer compared to isotope patterns of fragments from POPd2-Ad.

assumption and the theory employed by Martin et al.,[29] if the cation (K^+) was considered in the $R_2(K^+O^-)P \rightarrow Ni(CO)_3$ (R = ^{t}Bu and Ad) model, the extrapolated TEPs were calculated to be 2035 and 2032 cm^{-1}. Overall, the results indicated that (deprotonated) PA-Ad is a better electron donor than PA-tBu.

The steric effect of the different PA-R ligands substituted was again evaluated by the percent buried volume (%V_{bur}). Using the crystal structures of POPd-tBu[30,25b] and POPd-Ad, the %V_{bur} values were estimated to be 29.1% and 30.2%, respectively. As for POPd2-tBu[14a] and POPd2-Ad, the %V_{bur} values were estimated to be 32.1 and 32.5%, respectively. The steric effect because of the PA-Ad ligand was slightly larger than that due to PA-tBu. In terms of steric and electronic descriptors, PA-Ad can therefore be expected to be a suitable ligand for palladium.

POPd-Ad and POPd2-Ad as Precatalysts for Suzuki Cross-Coupling Reactions. POPd-Ad was utilized to test its potential as a precatalyst for the Suzuki reaction of phenyl chloride (Scheme 3). To identify the best combination of the solvent and base, initial experimental conditions included the use of 2 mol % of POPd-Ad, 0.5 mmol of aryl chloride, 0.55 mmol of 4-tolylboronic acid, and 3 equiv of base. The reaction

Scheme 3. Initial Reaction Condition Employed To Screen the Best Combination of the Base and Solvent for the Model Suzuki Reaction

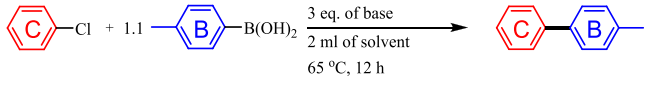

https://doi.org/10.1021/acsomega.1c06430
ACS Omega 2021, 6, 35134−35143

was conducted in 2 mL of solvent at 65 °C for 12 h while evaluating the effect of different solvents.

For the four solvents evaluated (toluene, THF, 1,4-dioxane, and acetonitrile) (Table 1 and Table S3), toluene and

Table 1. Search for an Optimized Set of Base and Solvent for POPd-Ad-Catalyzed Suzuki Reaction of Phenyl Chloride[a,b]

		solvent			
	base	toluene	THF	1,4-dioxane	ACN
1	KF	1	49	17	<1
2	K_2CO_3	2	11	32	<1
3	K_3PO_4	9	62	66	<1
4	KO^{t}Bu	44	91	91	ND
5	CsF	17	30	50	7
6	Cs_2CO_3	14	54	47	<1

[a]Reaction conditions: Phenyl chloride (0.5 mmol) and 4-tolylboronic acid (0.55 mmol) were employed as substrates. Reactions were carried out at 65 °C for 12 h. [b]Conversions (%) were determined by GC−MS.

acetonitrile were shown to not be suitable solvents for the Suzuki reaction, although six bases were examined for each (Tables 1 and S3). For THF and 1,4-dioxane, the best conversion yields (up to 91%) were obtained with KO^{t}Bu. To optimize the reaction time for the Suzuki reaction, further work was therefore focused on these two solvents. Here, the experiments indicated a marginal improvement in the reaction rate for 1,4-dioxane compared to that of THF over the first 3 h of the reaction (Table S4). Hence, 1,4-dioxane and KO^{t}Bu were selected as optimum solvents when employing POPd-Ad as the precatalyst.

A low gas chromatography−mass spectrometry (GC−MS) conversion (7%) was obtained when phenyl chloride was catalyzed with acetonitrile and CsF at 65 °C for 12 h (Scheme 3). However, when Ph-Br (62%) and Ph-OTf (32%) were used as the substrate while the same reaction conditions were employed, much higher isolated yields were obtained. This result agrees with previous results reported by Proutiere and Schoenebeck, indicating that the oxidative addition of the C−OTf bond to Pd(0) catalytic species in the presence of F^- or $ArB(OH)O^-$ in polar acetonitrile was preferable for the use of nonpolar THF.[31] This C−Cl or C−OTf bond preference may be due to the formation of coordinating anionic species ($ArB(OH)O^-$ or F^-) in polar solvents[31] and the related bis-ligated catalytic species.[32]

Finally, the Suzuki reactions of phenyl chloride and 1.1 equiv of 4-tolylboronic acid were carried out in 1,4-dioxane with KO^{t}Bu at either 85 or 95 °C (Table S5). After 2 h, the GC conversion yields were 68% at 85 °C and 75% at 95 °C. As a final optimization step, the amount of 4-tolylboronic acid was increased to 1.5 equiv, and this amount was reacted at 95 °C for 0.5 h, resulting in a conversion of 99% (Table S6). The results further indicated that the reactions were completed in 0.5 h. The optimized reaction conditions for the POPd-Ad precatalyst are summarized in Scheme 4.

Di-nuclear POPd1-tolyl is ligated by PA-Ph ($Ph_2(HO)P$:), with two smaller phenyl groups,[33] while mononuclear POPd-tBu,[34] di-nuclear POPd1-tBu, and POPd2-tBu[14a,34] are associated with bulky ^{t}Bu$_2$P-OH (PA-tBu) ligands. The latter precatalysts have previously been demonstrated to be effective precatalysts for Suzuki reactions of aryl chlorides.[14c] However,

Scheme 4. Optimized Reaction Conditions for POPd-Ad and POPd2-Ad-Catalyzed Suzuki Reaction

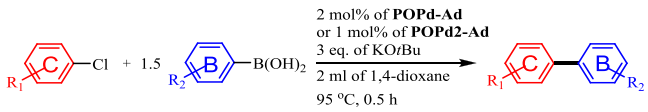

to achieve good catalytic yields, long reaction times were required. In this study, these four complexes were synthesized based on previously reported methods and subsequently used as precatalysts employing the optimized conditions determined for POPd-Ad (Table 2).

Table 2. Comparison of the Suzuki Reactions of Phenyl Chloride and 4-Tolylboronic Acid as Catalyzed Using Various Precatalysts[a,b]

entry	precatalyst	mol %	isolated yield (%)
1	POPd1-tolyl	1	15
2	POPd-tBu	2	72
3	POPd1-tBu	1	81
4	POPd2-tBu	1	70
5	POPd-Ad	2	99
6	POPd2-Ad	1	99

[a]Phenyl chloride (0.5 mmol) and 4-tolylboronic acid (0.75 mmol) were used as substrates. [b]The optimized reaction conditions are shown in Scheme 4.

As expected, the three PA-tBu-coordinated Pd(II) complexes were found to be satisfactory precatalysts (entries 2−4), although POPd1-tolyl was not effective. By employing the optimized reaction conditions, the reaction time for the POPd1-tBu-catalyzed Suzuki reaction could further be significantly reduced from 12 h (previously reported) to only 0.5 h.[14a] In addition, both POPd-Ad and POPd2-Ad were more efficient precatalysts than POPd1-tBu and POPd2-tBu, as shown by the quantitative conversion of phenyl chloride to 4-phenyltoluene (entries 5 and 6). Bis-ligated POPd-Ad was shown to be a less efficient precatalyst than monoligated POPd2-Ad.

Ligation State of Active Species in the Suzuki Cross-Coupling Reaction. To determine the influence of the amount of the SPO-Ad preligand on the catalytic yield of the Suzuki reaction shown in Scheme 3, excess SPO-Ad was added to the POPd2-Ad catalyzed Suzuki reaction of phenyl chloride and 4-tolylboronic acid (Table 3). Here, the use of excess preligands resulted in a reduction of the catalytic yield, with the yield associated with 4-phenyltoluene decreasing to only

Table 3. Determination of the Optimal Pd-to-SPO-Ad Ratio for the POPd-Ad-Catalyzed Suzuki Reaction of Phenyl Chloride and 4-Tolylboronic acid[a]

entry	POPd2-Ad (mol %)	SPO-Ad (mol %)	conversion yield[b] (%)
1	1	0	95
2		2	80
3		4	27
4		10	5

[a]Phenyl chloride (0.5 mmol), 4-tolylboronic acid (0.55 mmol), and 3 equiv of KO^{t}Bu; reaction in 2 mL of 1,4-dioxane at 65 °C for 12 h. [b]Determined by GC with a barrier discharge ionization detector (GC-BID).

https://doi.org/10.1021/acsomega.1c06430
ACS Omega 2021, 6, 35134−35143

5% when 10 mol % of SPO-Ad was added (entry 4: Pd:SPO-Ad = 1:5). These results indicated that the active species could be a mononuclear and monoligated Pd complex.

DFT Calculations and Temperature Effects on the Formation of Mono-Ligated Pd(II) Species. To gain insight into the differences between the Ad_2P-OH and $^tBu_2P$-OH ligands in catalysis, DFT calculations were performed to determine the ligand dissociation free energies for POPd-R (Figure 4) and the dimer-to-monomer process free energies for

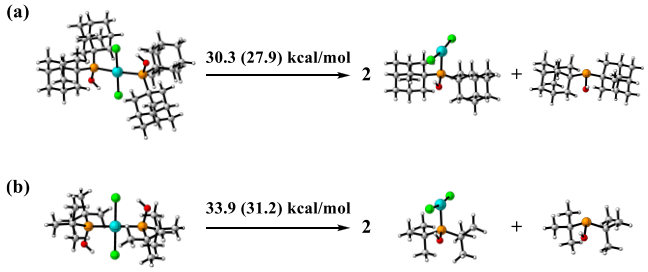

Figure 4. Gas-phase (solution) dissociation free energies for (a) POPd-Ad and (b) POPd-tBu (ωB97xD results, MWB28 pseudopotential and valence basis set for Pd, and 6-31G(d) for the other atoms. IEFPCM model was used to account for the solvation effect of 1,4-dioxane.).

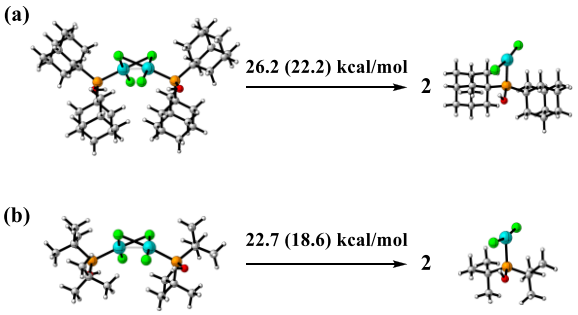

Figure 5. Gas-phase (solution) dissociation free energies for (a) POPd2-Ad and (b) POPd2-tBu (ωB97xD results, MWB28 pseudopotential and valence basis set for Pd, and 6-31G(d) for the other atoms. The IEFPCM model was used to account for the solvation effect of 1,4-dioxane).

POPd2-R (Figure 5). The most stable isomers identified were associated with species with two intramolecular hydrogen bonds between the two P−OH···Cl fragments, and these were consequently evaluated in further investigations (Figures S3−S5).

Here, the ωB97xD-optimized geometries of POPd-Ad (Figure 4a) and POPd-tBu (Figure 4b) well fit the structures determined by X-ray analysis. For POPd-tBu, the optimized (X-ray) bond lengths for the two Pd−P bonds are 2.370 Å (2.3450(3) Å), while they are 2.354 Å (2.3132(3) Å) for two Pd−Cl bonds.[30] Moreover, the two P−O bond lengths are 1.635 Å (1.6141(17) Å), with the two associated Cl−Pd−P angles being 88.3° (88.98(1)°). In the case of POPd-Ad, the optimized (X-ray) bond lengths for the two Pd−P bonds are 2.369 and 2.372 Å (2.3483(5) Å), and 2.356 and 2.358 Å (2.3082(6) Å) for the two Pd−Cl bonds.[30] Here, the two P−O bond lengths are 1.636 Å (1.6141(17) Å), and the two Cl−Pd−P angles are 88.3° (88.09(2)°).

Based on the X-ray structure reported for POPd2-tBu, it has a perfect planar Pd_2Cl_2 core.[14a] Calculations performed as part of this work did, however, indicate that this planar core is a transition state with an out-of-plane imaginary frequency of −7.97 cm^{-1} existing between two $PdCl_2(P(OH)^tBu_2)$ fragments. The observed planar Pd_2Cl_2 core could, therefore, have been a result of the solid-state packing force. The local minimum of POPd2-tBu is associated with a butterfly-shaped Pd_2Cl_2 core (Figure 5b). Both the X-ray structure and DFT-optimized geometry for $POPd_2$-Ad confirmed this proposed geometry (Figure 5a and Table S1). The butterfly-shaped Pd_2Cl_2 core in POPd2-tBu and POPd2-Ad could be due to the steric hindrance between the two adjacent $^tBu_2P$-OH and Ad_2P-OH ligands. The optimized (X-ray) Pd···Pd distances for POPd2-tBu and POPd2-Ad are 3.110 and 3.068 Å (3.046(3) Å), respectively, with Pd−P distances for POPd2-tBu and POPd2-Ad being 2.270/2.272 and 2.262 Å (2.235(6) and 2.236(8) Å), respectively. The two Pd−Cl distances associated with the connection of two $R_2(OH)P \rightarrow Pd(II)Cl_2$ fragments for POPd2-tBu 2.467 and 2.468 Å, compared to the associated Pd-Cl distances of 2.475 Å (2.452(8) and 2.466(9) Å) for POPd2-Ad, respectively. Because of their different core geometries, the X-ray structure of POPd2-tBu was not compared with its optimized counterpart.

The bond dissociation free energies of PA-R for POPd-Ad and POPd-tBu in 1,4-dioxane were estimated to be 27.9 and 31.2 kcal/mol, respectively (Figure 4), indicating that the dissociation of PA-Ad from the Pd(II) center to form monoligated and mononuclear Pd species would be easier than that for PA-tBu. In contrast, the two dimer-to-monomer dissociation free energies of POPd2-Ad and POPd2-tBu were estimated to be 22.2 and 18.6 kcal/mol, respectively (Figure 5). As indicated by the interaction region indicator (IRI),[35] the smaller bond dissociation free energy of POPd-Ad, when compared to that of POPd-tBu, may originate from the stronger steric repulsion between two closely contacted adamantyl groups when attached to two different PA ligands (Figure S6a,b). Here, the two adamantyl units in the mononuclear POPd-Ad are closer to each other than in the di-nuclear POPd2-Ad. IRI analyses further indicated that the larger dimer-to-monomer free energy of POPd2-Ad, compared to that of POPd2-tBu, might be due to van der Waals interactions between the two adamantyl groups attached to two different PA ligands (Figure S6c,d).

Considering that the ligated $R_2(HO)P$ is a deprotonatable ligand, the dissociation free energies for the singly deprotonated POPd-R ($R_2(^-O)P \rightarrow PdCl_2 \leftarrow P(OH)R_2$) and the dimer-to-mono process for the deprotonated POPd2-R ($(R_2(^-O)P \rightarrow PdCl)(\mu\text{-}Cl)_2$ ($PdCl \leftarrow P(OH)R_2$)) in 1,4-dioxane were calculated (Figures S7 and S8). In Figure S7, the isomers with the best stability were also compared. For the singly deprotonated POPd-Ad (Figure S7a) and POPd-tBu (Figure S7b), the ligand dissociation free energies of PA-R in 1,4-dioxane were 9.5 and 11.7 kcal/mol, while the dissociation free energies associated with the breaking dimer for deprotonated POPd2-Ad and POPd2-tBu in 1,4-dioxane were 15.3 and 12.1 kcal/mol (Figure S8), respectively. The smaller free energies required for the dissociation of the singly deprotonated POPd-R and POPd2-R, when compared to that of their neutral counterparts, may be due to the stronger trans effect of the deprotonated $R_2(^-O)P$ ligand. Notably, the resultant deprotonated mono-PA-ligated and mononuclear $Cl_2Pd(II) \rightarrow P(O^-)Ad_2$ species is the ionic species B detected

https://doi.org/10.1021/acsomega.1c06430
ACS Omega 2021, 6, 35134−35143

in the ESI$^-$ mass spectrum of POPd2-Ad. In addition, the negative dissociation free energies calculated for the fully deprotonated POPd-R (ligand dissociation) and POPd2-R (dimer-to-monomer process) in 1.4-dioxane indicated that these were spontaneous reactions (Figures S11 and S12).

By employing phenyl chloride and 4-tolylboronic acid as substrates in the Suzuki reaction, the reaction temperature of 95 °C was lowered to study the ligation state of POPd-Ad and POPd2-Ad (Table S7). At 45 and 55 °C, the respective GC yields of the POPd-Ad-catalyzed Suzuki reaction were 3 and 54%, respectively. Compared to this, GC yields of the POPd2-Ad catalyzed reaction were 10 and 83% at 45 and 55 °C, respectively. This indicated that POPd2-Ad performed better as a precatalyst when compared to POPd-Ad. In addition, the dissociation of the PA-R ligand from POPd-R became unfavorable at lower temperatures, while the dissociated PA-R further reduced the catalytic yield. (Table 3). These resultant species could be monoligated and mononuclear $R_2(^-O)P \rightarrow Pd(II)Cl_2$ for both precatalysts. It should further be considered that the ligand dissociation free energies for the singly deprotonated POPd-Ad and POPd2-tBu are 9.5 and 11.7 kcal/mol, respectively. Combined with the larger electronic and steric effects associated with PA-Ad when compared to PA-tBu, this supported the conclusion that POPd-Ad would be a better precatalyst than POPd-tBu (entries 2 and 5 in Table 2).

Nonetheless, in 1,4-dioxane, the dimer-to-monomer free energy of the singly deprotonated PAPd2-Ad (15.3 kcal/mol) was found to be larger than the ligand dissociation free energy of the singly deprotonated POPd-Ad (9.5 kcal/mol). The energy required for the formation of $R_2(^-O)P \rightarrow Pd(II)Cl_2$ therefore appeared to be contradictory to the catalytic yields observed at 45 and 55 °C. Table 3 further shows that the best Pd-to-PA ratio is 1:1, with yields being significantly affected by the redundant ligands, as seen in the low yield of the POPd-Ad-catalyzed Suzuki reaction at 45 and 55 °C. At 95 °C, the catalytic performances of POPd-Ad and POPd2-Ad were comparable (entries 5 and 6 in Table 2). This would indicate that elevated temperatures prevent the re-coordination of extra $Ad_2(HO)P$ or $Ad_2(^-O)P$ ligands in POPd-Ad-catalyzed Suzuki reactions.

Reduction of Pd(II) Precatalysts. Potential reduction pathways of Pd(II) in POPd-Ad and POPd2-Ad were also investigated (Scheme 5, results listed in Table 4). Here, either POPd-Ad or POPd2-Ad was reacted in 1,4-dioxane with four equiv of 4-tolylbronic acid and 30 equiv of KO^{t}Bu at 95 °C for 0.5 h. Three products were obtained from these reactions. First, the formation of 4,4′-dimethyl-1,1′-biphenyl may be associated with the reduction of Pd(II) by 4-tolylbronic acid in either POPd-Ad or POPd2-Ad.[36] The isolation of phosphine oxide further indicated that Pd(II) in the precatalyst was reduced through C_{tolyl}-P(=O)Ad_2 bond coupling. This agrees with a reductive elimination reaction via C−P bond formation between the deprotonated SPO-R and the aryl group of the aryl-Pd(II)-P(O^-)R_2 species, as has been reported in the literature.[37] Finally, the dissociation of PA-Ad may be assumed, where SPO-Ad could be isolated, although the decomposition of Pd species cannot be excluded as a possible mechanism.

Scheme 5. Reaction between the POPd-Ad and POPd2-Ad with 4-Tolylboronic Acid in the Presence of 30 equiv of KO^{t}Bu at 95 °C for 0.5 h

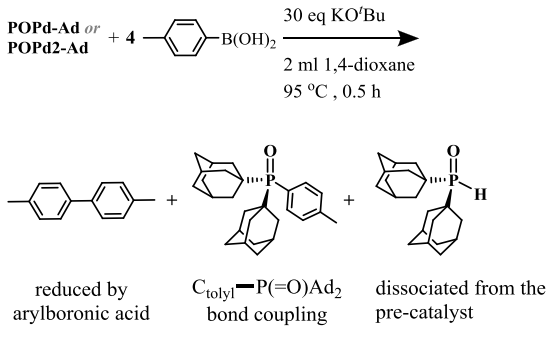

Table 4. Reaction between the POPd-Ad or POPd2-Ad with 4-Tolylboronic Acid in the Presence of 30 equiv of KO^{t}Bu[a,b]

	precatalyst	biphenyl (%)	phosphine oxide (%)	SPO-Ad (%)
1	POPd-Ad	14	ND	30
2	POPd2-Ad	73	ND	5

[a]See Scheme 5 for the detailed reaction condition. [b]Isolated yield.

After the reaction shown in Scheme 5 was completed, 4,4′-dimethyl-1,1′-biphenyl was isolated. With no evidence of the formation of phosphine oxide (Tables 4 and S8), boronic acid was assumed to be the reducing agent in the reduction of Pd(II) in POPd-Ad and POPd2-Ad. SPO-Ad could further be isolated from both POPd-Ad (30%) and POPd2-Ad (5%). These results imply that the dissociation of PA-Ad from bis-ligated and mononuclear POPd-Ad is crucial to form monoligated Pd(0) active species. Alternatively, this could also represent the decomposition of the reduced Pd(0) active species. However, it is believed that most SPO-Ad dissociated from POPd-Ad to form the monoligated and mononuclear species at 95 °C. This is supported by the fact that only 5% of SPO-Ad was recovered when the dimer-to-monomer process of $POPd_2$-Ad was conducted under the same reaction conditions employed for POPd-Ad.

Yields of 4,4′-dimethyl-1,1′-biphenyl were 14 and 73% for POPd-Ad and POPd2-Ad, respectively. For POPd-Ad, the low yield could be attributed to the bis-ligated nature of the precatalyst, while the dissociated SPO-Ad could also recoordinate to the Pd(II) center to slow down the rate of the Pd(II) reduction of POPd-Ad. Regarding POPd2-Ad, the higher yield may be associated with the monoligated Pd(II) species formed after the dimer-to-monomer process of POPd2-Ad.

Application of POPd-Ad and POPd2-Ad to Other Aryl Chlorides. To examine the applicability and functional group tolerance of the substrates, POPd2-Ad was employed as a precatalyst in the Suzuki reaction (Figure 6). The use of electron-deficient 4-(trifluoromethyl)phenylboronic acid resulted in a low yield (**c**: 31%).[38] Comparing the yields of products **a**−**c**, the use of 4-tolylboronic acid (**b**) was associated with the best result.[38] However, poor yields were obtained when a sterically congested arylboronic acid was selected as a substrate [**e** (99%) versus **f** (27%)]. Considering the yields of products **a**, **d**, **e**, **g**, **h**, and **i**, increasing the steric hindrance on the 2- and/or 6-position of aryl chlorides appears not to influence the yields significantly. This would imply that the oxidative addition of aryl chlorides to the Pd(0) active species proceeded smoothly. Data for **g** (81%), **h** (71%), and **j** (78%)-**k** (71%) revealed the same trend. Comparing the yields of **i** (74%) and **l** (24%), the low yield of **l** could be related to the

https://doi.org/10.1021/acsomega.1c06430
ACS Omega 2021, 6, 35134−35143

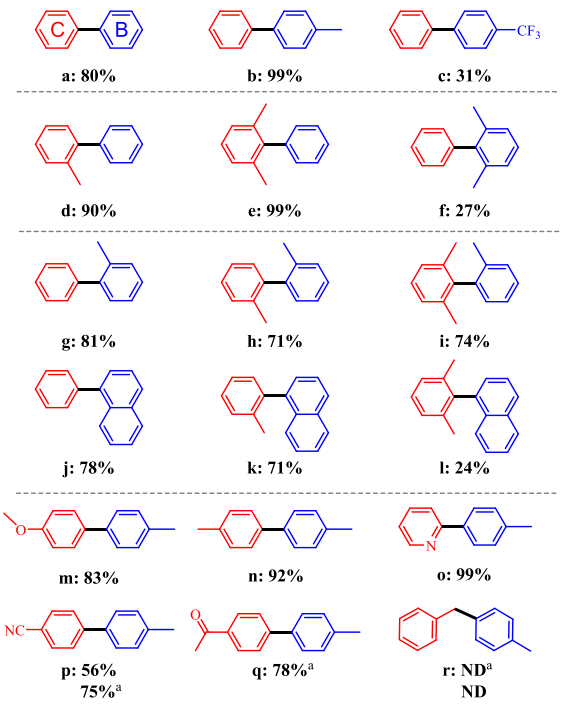

Figure 6. POPd2-Ad-catalyzed Suzuki reactions of various aryl chlorides and boronic acids carried out employing the optimized reaction conditions. Isolated yields were reported. [a]Three equivalents of CsF were used as the base. The duration of these reactions was 1 h.

synergy between steric and electronic effects of naphthalen group. Considering both the electronic and steric effects associated with the yields associated with arylboronic acids, the transmetalation may be assumed to be the rate-limiting step.[39]

Good yields of products **m** (83%) and **n** (92%) were further observed where the electron-donating group was functionalized on the 4-position of phenyl chloride (Figure 6). For heteroatom-substituted 2-chloropyridine, a yield of 99% was obtained (**o**). The use of 2-chloropyridine in POPd2-Ad catalyzed Suzuki reaction could therefore be proposed as an alternative route to overcome the problematic protodeboronation of 2-pyridyl boronic acid.[40] For 4-chlorobenzonitrile, the yield of 4-cyano-4′-methylbiphenyl was found to be 56% (**p**), while no conversion of 4-chloroacetophenone (**q**) was observed. This could be related to the use of $^{-}O^{t}Bu$. CsF was subsequently used to replace $KO^{t}Bu$ in the two reactions, where, after only 1 h, yields of **p** and **q** increased to 75 and 78%, respectively. No conversion was observed when benzyl chloride was used as the substrate.

Reaction Mechanism. Li et al. reported that $^{t}Bu_2(O^{-})P \rightarrow Pd(0) \leftarrow P(O^{-})^{t}Bu_2$ or anionic $^{t}Bu_2(O^{-})P \rightarrow Pd(0)Cl \leftarrow P(O^{-})^{t}Bu_2$ could precipitate when POPd1-tBu was reacted with a base.[14b] Here, it was, however, assumed that the transmetalation reaction between the Pd(II) species and aryl boronic acid could also occur after the di-nuclear POPd2-Ad dissociated into two mononuclear $Cl_2Pd(II) \leftarrow P(OH)Ad_2$ or deprotonated $Cl_2Pd(II) \leftarrow P(O^{-})Ad_2$ species (species B detected in the ESI^{-} mass spectrum of POPd2-Ad).[41] In addition, for the mononuclear POPd-Ad, one bulky PA-Ad could initially dissociate from the Pd(II) center to form the same mononuclear Pd(II) species.

It was determined that when the base was reacted with POPd1-Ph ($(Ph_2(HO)P)_2PdCl_2$), the deprotonation of $R_2(HO)P$ occurred to yield polymeric $(Ph_2(^{-}O)P)_2Pd(II)$.[15] Therefore, an anionic mononuclear $Cl_2Pd(II) \leftarrow P(O^{-})Ad_2$ was proposed when the base was reacted with POPd-Ad and POPd2-Ad. Subsequently, an anionic (4-tolyl)-ClPd(II) $\leftarrow P(O^{-})Ad_2$ intermediate could be formed through a base-assisted transmetalation reaction with 4-tolylboronic acid. The reduction of Pd(II) would then proceed via a second base-assisted transmetalation reaction between boronic acid and the (4-tolyl)-ClPd(II)-P(=O)Ad_2 intermediate to yield $(4\text{-tolyl})_2$-Pd(II)-P(=O)Ad_2 species. Following the reductive elimination of 4,4′-dimethyl-1,1′-biphenyl, the anionic and zero-valent active species of Pd(0) $\leftarrow P(O^{-})Ad_2$ would then be formed (Figure 7), where the electron-rich anionic $P(O^{-})Ad_2$ could

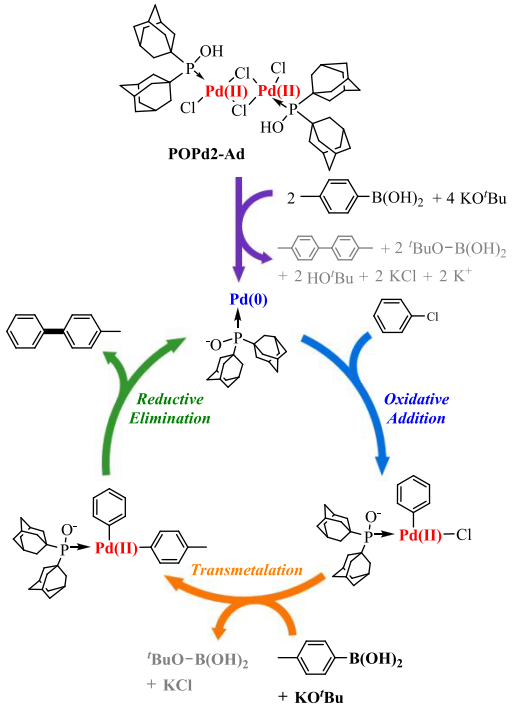

Figure 7. Proposed Suzuki reaction mechanism as catalyzed by the POPd2-Ad. The graphical representation of the catalytic cycle was generated using the catalytic cycle generator.[42,43]

facilitate the oxidative addition of unreactive aryl chlorides. Based on the results obtained in this study, the proposed reaction mechanism for the POPd-Ad- and POPd2-Ad-catalyzed Suzuki reaction of aryl chloride is shown in Figure 7.

CONCLUSIONS

In this study, POPd-Ad and POPd2-Ad were synthesized for the first time. The di-nuclear POPd2-Ad could be easily converted into two mononuclear POPd-Ad monomers in acetonitrile. POPd-Ad could also be obtained from the reaction of POPd2-Ad and SPO-Ad. It was shown that both POPd-Ad and POPd2-Ad complexes were useful precatalysts for Suzuki cross-coupling reactions of aryl chlorides in only 0.5 h. The potential reduction pathway and the ligation state for POPd-Ad as well as POPd2-Ad were investigated, showing that the Pd(0) active species was reduced by arylboronic acid. Here, the monoligated Pd(0) $\leftarrow P(O^{-})Ad_2$ was proposed to be the active species. DFT calculations and experimental data showed that the dissociation of the redundant PA-Ad ligand had a negative impact on the performance of the overall reaction when POPd-Ad was employed. Therefore, POPd2-Ad

https://doi.org/10.1021/acsomega.1c06430
ACS Omega 2021, 6, 35134−35143

was considered a better precatalyst than POPd-Ad. A catalytic reaction mechanism was further proposed. Employing the optimized reaction conditions obtained here, the reaction time required for POPd-tBu-, POPd1-tBu-, and POPd2-tBu-catalyzed Suzuki reactions could be significantly reduced from 12 h to approximately 0.5 h. These PA-Ad-ligated Pd(II) complexes will complement current research on the POPd series of precatalysts.

EXPERIMENTAL SECTION

The experimental and computational methods, characterizations, NMR spectra, and optimized coordinates are thoroughly detailed in the Supporting Information.

ASSOCIATED CONTENT

Supporting Information

The Supporting Information is available free of charge at https://pubs.acs.org/doi/10.1021/acsomega.1c06430.

Full experimental methods, characterization data, and NMR spectra of products from the Suzuki reactions (PDF)

Details of the optimized coordinates complied in a single XYZ-format file (XYZ)

Crystallographic information file of POPd-Ad (CCDC 1994915) (CIF)

Crystallographic information file of POPd2-Ad (CCDC 1994919) (CIF)

AUTHOR INFORMATION

Corresponding Author

Yu-Chang Chang − *Department of Applied Chemistry, Providence University, Taichung City 43301, Taiwan;* orcid.org/0000-0003-1516-7658; Email: vickchang@pu.edu.tw

Authors

He-Xin Xiao − *Department of Applied Chemistry, Providence University, Taichung City 43301, Taiwan;* orcid.org/0000-0002-9043-0041

Wan-Yun Hsu − *Department of Applied Chemistry, Providence University, Taichung City 43301, Taiwan;* orcid.org/0000-0002-5909-6209

Siou-Wei Liang − *Department of Applied Chemistry, Providence University, Taichung City 43301, Taiwan*

Yingjie Guo − *Department of Cosmetic Science, Providence University, Taichung City 43301, Taiwan;* orcid.org/0000-0003-0112-7145

Wan-Ching Lee − *Department of Chemistry, National Chung Hsing University, Taichung City 40227, Taiwan*

I-Chung Lu − *Department of Chemistry, National Chung Hsing University, Taichung City 40227, Taiwan;* orcid.org/0000-0002-3125-6397

Complete contact information is available at: https://pubs.acs.org/10.1021/acsomega.1c06430

Notes

The authors declare no competing financial interest.

ACKNOWLEDGMENTS

Financial support from the Ministry of Science and Technology, Taiwan (MOST), is appreciated (MOST 107-2113-M-126-002-MY2, MOST 109-2113-M-126-004-MY2). We express our gratitude to the Providence University for supporting this research (PU106-11100-C01). We are also grateful to the National Center for High-Performance Computing for computing time and facilities. We thank Mr. Tzu-Hao Lin for performing the ^{31}P NMR experiments with an attempt to observe the formation of plausible Pd(0) species.

REFERENCES

(1) (a) Heravi, M. M.; Hashemi, E. Recent applications of the Suzuki reaction in total synthesis. *Tetrahedron* **2012**, *68*, 9145−9178. (b) Taheri Kal Koshvandi, A.; Heravi, M.; Momeni, T. Current applications of Suzuki-Miyaura coupling reaction in the total synthesis of natural products: an update: applications of Suzuki-Miyaura coupling reaction in natural products. *Appl. Organomet. Chem.* **2018**, *32*, No. e4210.

(2) (a) Suzuki, A. Recent advances in the cross-coupling reactions of organoboron derivatives with organic electrophiles, 1995−1998. *J. Organomet. Chem.* **1999**, *576*, 147−168. (b) Schiedel, M. S.; Briehn, C. A.; Bäuerle, P. C-C cross-coupling reactions for the combinatorial synthesis of novel organic materials. *J. Organomet. Chem.* **2002**, *653*, 200−208. (c) Babudri, F.; Farinola, G. M.; Naso, F. Synthesis of conjugated oligomers and polymers: The organometallic way. *J. Mater. Chem.* **2004**, *14*, 11−34.

(3) (a) Keaveney, S. T.; Schoenebeck, F. Palladium-catalyzed decarbonylative trifluoromethylation of acid fluorides. *Angew. Chem., Int. Ed.* **2018**, *57*, 4073−4077. (b) Wang, Z.; Wang, X.; Nishihara, Y. Nickel-catalysed decarbonylative borylation of aroyl fluorides. *Chem. Commun.* **2018**, *54*, 13969−13972. (c) Malapit, C. A.; Bour, J. R.; Laursen, S. R.; Sanford, M. S. Mechanism and scope of nickel-catalyzed decarbonylative borylation of carboxylic acid fluorides. *J. Am. Chem. Soc.* **2019**, *141*, 17322−17330. (d) Wang, X.; Wang, Z.; Nishihara, Y. Nickel/copper-cocatalyzed decarbonylative silylation of acyl fluorides. *Chem. Commun.* **2019**, *55*, 10507−10510. (e) Fu, L.; Chen, Q.; Wang, Z.; Nishihara, Y. Palladium-Catalyzed Decarbonylative Alkylation of Acyl Fluorides. *Org. Lett.* **2020**, *22*, 2350−2353.

(4) (a) Liu, C.; Szostak, M. Decarbonylative phosphorylation of amides by palladium and nickel catalysis: the Hirao cross-coupling of amide derivatives. *Angew. Chem., Int. Ed.* **2017**, *56*, 12718−12722. (b) Shi, S.; Szostak, M. Decarbonylative cyanation of amides by palladium catalysis. *Org. Lett.* **2017**, *19*, 3095−3098. (c) Shi, S.; Szostak, M. Decarbonylative borylation of amides by palladium catalysis. *ACS Omega* **2019**, *4*, 4901−4907. (d) Zhou, T.; Ji, C.-L.; Hong, X.; Szostak, M. Palladium-catalyzed decarbonylative Suzuki−Miyaura cross-coupling of amides by carbon−nitrogen bond activation. *Chem. Sci.* **2019**, *10*, 9865−9871.

(5) (a) Ben Halima, T.; Zhang, W.; Yalaoui, I.; Hong, X.; Yang, Y.-F.; Houk, K. N.; Newman, S. G. Palladium-catalyzed Suzuki−Miyaura coupling of aryl esters. *J. Am. Chem. Soc.* **2017**, *139*, 1311−1318. (b) Buchspies, J.; Szostak, M. Recent advances in acyl suzuki cross-coupling. *Catalysts* **2019**, *9*, 53. (c) Zhou, T.; Li, G.; Nolan, S. P.; Szostak, M. Well-defined, air-stable, and readily available precatalysts for suzuki and Buchwald-Hartwig cross-coupling (transamidation) of amides and esters by N-C/O-C Activation. *Org. Lett.* **2019**, *21*, 3304−3309. (d) Li, G.; Zhou, T.; Poater, A.; Cavallo, L.; Nolan, S. P.; Szostak, M. Buchwald-Hartwig cross-coupling of amides (transamidation) by selective N-C(O) cleavage mediated by air- And moisture-stable [Pd(NHC)(allyl)Cl] precatalysts: Catalyst evaluation and mechanism. *Catal. Sci. Technol.* **2020**, *10*, 710−716.

(6) (a) Blanchard, N.; Bizet, V. Acid Fluorides in Transition-Metal Catalysis: A Good Balance between Stability and Reactivity. *Angew. Chem., Int. Ed.* **2019**, *58*, 6814−6817. (b) Ogiwara, Y.; Sakai, N. Acyl fluorides in late-transition-metal catalysis. *Angew. Chem., Int. Ed.* **2020**, *59*, 574−594.

(7) Gildner, P. G.; Colacot, T. J. Reactions of the 21st century: Two decades of innovative catalyst design for palladium-catalyzed cross-couplings. *Organometallics* **2015**, *34*, 5497−5508.

(8) (a) Lundgren, R. J.; Stradiotto, M. Addressing challenges in palladium-catalyzed cross-coupling reactions through ligand design.

Chem. – Eur. J. **2012**, *18*, 9758–9769. (b) Lundgren, R. J.; Stradiotto, M., Key Concepts in ligand design. In *Ligand Design in Metal Chemistry*, 2016, 1–14.
(9) (a) Martin, R.; Buchwald, S. L. Palladium-catalyzed suzuki-miyaura cross-coupling reactions employing dialkylbiaryl phosphine ligands. *Acc. Chem. Res.* **2008**, *41*, 1461–1473. (b) Stradiotto, M.; Lundgren, R. J.Application of sterically demanding phosphine ligands in palladium-catalyzed cross-coupling leading to C(sp2)-E bond formation (E = NH2, OH, and F). In *Ligand Design in Metal Chemistry*, 2016; 104–133.
(10) (a) Lyn Farmer, J.; Pompeo, M.; Organ, M. G.Pd-N-heterocyclic carbene complexes in cross-coupling applications. In *Ligand Design in Metal Chemistry*, 134–175; (b) Hillier, A. C.; Grasa, G. A.; Viciu, M. S.; Lee, H. M.; Yang, C.; Nolan, S. P. Catalytic cross-coupling reactions mediated by palladium/nucleophilic carbene systems. *J. Organomet. Chem.* **2002**, *653*, 69–82. (c) Würtz, S.; Glorius, F. Surveying sterically demanding n-heterocyclic carbene ligands with restricted flexibility for palladium-catalyzed cross-coupling reactions. *Acc. Chem. Res.* **2008**, *41*, 1523–1533.
(11) (a) Hsu, Y.-C.; Shen, J.-S.; Lin, B.-C.; Chen, W.-C.; Chan, Y.-T.; Ching, W.-M.; Yap, G. P. A.; Hsu, C.-P.; Ong, T.-G. Synthesis and Isolation of an Acyclic Tridentate Bis(pyridine)carbodicarbene and Studies on Its Structural Implications and Reactivities. *Angew. Chem., Int. Ed.* **2015**, *54*, 2420–2424. (b) Wang, T.-H.; Chen, W.-C.; Ong, T.-G. Carbodicarbenes or bent allenes. *J. Chin. Chem. Soc.* **2017**, *64*, 124–132. (c) Hsu, Y.-C.; Wang, V. C.-C.; Au-Yeung, K.-C.; Tsai, C.-Y.; Chang, C.-C.; Lin, B.-C.; Chan, Y.-T.; Hsu, C.-P.; Yap, G. P. A.; Jurca, T.; Ong, T.-G. One-pot tandem photoredox and cross-coupling catalysis with a single palladium carbodicarbene complex. *Angew. Chem., Int. Ed.* **2018**, *57*, 4622–4626. (d) Liu, S.-K.; Shih, W.-C.; Chen, W.-C.; Ong, T.-G. Carbodicarbenes and their captodative behavior in catalysis. *ChemCatChem* **2018**, *10*, 1483–1498. (e) Ambre, R.; Yang, H.; Chen, W.-C.; Yap, G. P. A.; Jurca, T.; Ong, T.-G. Nickel carbodicarbene catalyzes kumada cross-coupling of aryl ethers with grignard reagents through C–O bond activation. *Eur. J. Inorg. Chem.* **2019**, *2019*, 3511–3517.
(12) (a) Nemoto, T.; Hamada, Y. Catalytic asymmetric synthesis using P-chiral diaminophosphine oxide preligands: DIAPHOXs. *Tetrahedron* **2011**, *67*, 667–687. (b) Shaikh, T. M.; Weng, C. M.; Hong, F. E. Secondary phosphine oxides: Versatile ligands in transition metal-catalyzed cross-coupling reactions. *Coord. Chem. Rev.* **2012**, *256*, 771–803.
(13) (a) Achard, T.; Giordano, L.; Tenaglia, A.; Gimbert, Y.; Buono, G. Steric control in the synthesis of phosphinous acid-coordinated mono- and binuclear platinum(ii) complexes. *Organometallics* **2010**, *29*, 3936–3950. (b) Vasseur, A.; Membrat, R.; Gatineau, D.; Tenaglia, A.; Nuel, D.; Giordano, L. Secondary phosphine oxides as multitalented preligands en route to the chemoselective palladium-catalyzed oxidation of alcohols. *ChemCatChem* **2017**, *9*, 728–732.
(14) (a) Li, G. Y. the first phosphine oxide ligand precursors for transition metal catalyzed cross-coupling reactions: C–C, C–N, and C–S bond formation on unactivated aryl chlorides. *Angew. Chem., Int. Ed.* **2001**, *40*, 1513–1516. (b) Li, G. Y.; Zheng, G.; Noonan, A. F. Highly active, air-stable versatile palladium catalysts for the C–C, C–N, and C–S bond formations via cross-coupling reactions of aryl chlorides. *J. Org. Chem.* **2001**, *66*, 8677–8681. (c) Li, G. Y. Highly active, air-stable palladium catalysts for the C–C and C–S bond-forming reactions of vinyl and aryl chlorides: Use of commercially available [(t-Bu)2P(OH)]2PdCl2, [(t-Bu)2P(OH)PdCl2]2, and [[(t-Bu)2PO···H···OP(t-Bu)2]PdCl]2 as catalysts. *J. Org. Chem.* **2002**, *67*, 3643–3650.
(15) Pryjomska, I.; Bartosz-Bechowski, H.; Ciunik, Z.; Trzeciak, A. M.; Ziółkowski, J. J. Chemistry of palladium phosphinite (PPh2(OR)) and phosphonite (P(OPh)2(OH)) complexes: Catalytic activity in methoxycarbonylation and Heck coupling reactions. *Dalton Trans.* **2006**, *213-220*, 213.
(16) (a) Roundhill, D. M.; Sperline, R. F.; Beaulied, W. B. Metal complexes of substituted phosphinites and secondary phosphites. *Coord. Chem. Rev.* **1978**, *26*, 263–279. (b) Walther, B. The coordination chemistry of secondary phosphine chalcogenides and their conjugate bases. *Coord. Chem. Rev.* **1984**, *60*, 67–105. (c) Appleby, T.; Derek Woollins, J. Inorganic backbone phosphines. *Coord. Chem. Rev.* **2002**, *235*, 121–140. (d) Gallen, A.; Riera, A.; Verdaguer, X.; Grabulosa, A. Coordination chemistry and catalysis with secondary phosphine oxides. *Catal. Sci. Technol.* **2019**, *9*, 5504–5561.
(17) Morgan, B. P.; Galdamez, G. A.; Gilliard, R. J., Jr; Smith, R. C. Canopied trans-chelating bis(N-heterocyclic carbene) ligand: Synthesis, structure and catalysis. *Dalton Trans.* **2009**, *2020-2028*, 2020.
(18) Graux, L. V.; Giorgi, M.; Buono, G.; Clavier, H. Ruthenium carbonyl complexes bearing secondary phosphine oxides and phosphinous acids: synthesis, characterization, and application in catalysis. *Organometallics* **2015**, *34*, 1864–1871.
(19) (a) Wolf, C.; Lerebours, R. Efficient Stille cross-coupling reaction using aryl chlorides or bromides in water. *J. Org. Chem.* **2003**, *68*, 7551–7554. (b) Wolf, C.; Lerebours, R. Use of highly active palladium-phosphinous acid catalysts in stille, heck, amination, and thiation reactions of chloroquinolines. *J. Org. Chem.* **2003**, *68*, 7077–7084. (c) Bigeault, J.; Giordano, L.; Buono, G. [2+1] cycloadditions of terminal alkynes to norbornene derivatives catalyzed by palladium complexes with phosphinous acid ligands. *Angew. Chem., Int. Ed.* **2005**, *44*, 4753–4757. (d) Wolf, C.; Xu, H. Efficient synthesis of sterically crowded biaryls by palladium-phosphinous acid-catalyzed cross-coupling of aryl halides and aryl Grignards. *J. Org. Chem.* **2008**, *73*, 162–167. (e) Xu, H.; Ekoue-Kovi, K.; Wolf, C. Palladium–phosphinous acid-catalyzed cross-coupling of aryl and acyl halides with aryl-, alkyl-, and vinylzinc reagents. *J. Org. Chem.* **2008**, *73*, 7638–7650. (f) Ackermann, L.; Vicente, R.; Hofmann, N. Air-stable secondary phosphine oxide as preligand for palladium-catalyzed intramolecular α-arylations with chloroarenes. *Org. Lett.* **2009**, *11*, 4274–4276. (g) Ackermann, L.; Potukuchi, H. K.; Kapdi, A. R.; Schulzke, C. Kumada–Corriu cross-couplings with 2-pyridyl grignard reagents. *Chem. – Eur. J.* **2010**, *16*, 3300–3303. (h) Chang, Y.-C.; Chang, W.-C.; Hu, C.-Y.; Hong, F.-E. Alkyl(quinolin-8-yl)phosphine oxides as hemilabile preligands for palladium-catalyzed reactions. *Organometallics* **2014**, *33*, 3523–3534. (i) Ghorai, D.; Müller, V.; Keil, H.; Stalke, D.; Zanoni, G.; Tkachenko, B. A.; Schreiner, P. R.; Ackermann, L. Secondary phosphine oxide preligands for palladium-catalyzed c–h (hetero)arylations: efficient access to pybox ligands. *Adv. Synth. Catal.* **2017**, *359*, 3137–3141.
(20) Ackermann, L.; Barfüsser, S.; Kornhaass, C.; Kapdi, A. R. C-H bond arylations and benzylations on oxazol(in)es with a palladium catalyst of a secondary phosphine oxide. *Org. Lett.* **2011**, *13*, 3082–3085.
(21) (a) Ackermann, L. Phosphine oxides as preligands in ruthenium-catalyzed arylations via C–H bond functionalization using aryl chlorides. *Org. Lett.* **2005**, *7*, 3123–3125. (b) Ackermann, L.; Vicente, R.; Althammer, A. assisted ruthenium-catalyzed c–h bond activation: carboxylic acids as cocatalysts for generally applicable direct arylations in apolar solvents. *Org. Lett.* **2008**, *10*, 2299–2302.
(22) Ackermann, L.; Born, R.; Spatz, J. H.; Meyer, D. Efficient aryl-(hetero)aryl coupling by activation of C-Cl and C-F bonds using nickel complexes of air-stable phosphine oxides. *Angew. Chem., Int. Ed.* **2005**, *44*, 7216–7219.
(23) (a) Poater, A.; Cosenza, B.; Correa, A.; Giudice, S.; Ragone, F.; Scarano, V.; Cavallo, L. SambVca: A web application for the calculation of the buried volume of N-heterocyclic carbene ligands. *Eur. J. Inorg. Chem.* **2009**, *2009*, 1759–1766. (b) Clavier, H.; Nolan, S. P. Percent buried volume for phosphine and N-heterocyclic carbene ligands: steric properties in organometallic chemistry. *Chem. Commun.* **2010**, *46*, 841–861.
(24) https://www.molnac.unisa.it/OMtools/sambvca2.1/index.html
(25) (a) Schröder, F.; Tugny, C.; Salanouve, E.; Clavier, H.; Giordano, L.; Moraleda, D.; Gimbert, Y.; Mouriès-Mansuy, V.; Goddard, J.-P.; Fensterbank, L. Secondary phosphine oxide–gold(I) complexes and their first application in catalysis. *Organometallics* **2014**, *33*, 4051–4056. (b) Graux, L. V.; Giorgi, M.; Buono, G.; Clavier, H. [RuCl(2)(eta(6)-p-cymene)] complexes bearing phosphi-

https://doi.org/10.1021/acsomega.1c06430
ACS Omega 2021, 6, 35134–35143

nous acid ligands: preparation, application in C-H bond functionalization and mechanistic investigations. *Dalton Trans.* **2016**, *45*, 6491−6502.
(26) Falivene, L.; Cao, Z.; Petta, A.; Serra, L.; Poater, A.; Oliva, R.; Scarano, V.; Cavallo, L. Towards the online computer-aided design of catalytic pockets. *Nat. Chem.* **2019**, *11*, 872−879.
(27) Chen, L.; Ren, P.; Carrow, B. P. Tri(1-adamantyl)phosphine: expanding the boundary of electron-releasing character available to organophosphorus compounds. *J. Am. Chem. Soc.* **2016**, *138*, 6392−6395.
(28) The average bond distance of Pd(II)-P(OH)R2 is 2.2498 angstrom. The structural search was done with Conquest Version 2.0.4 using the CSD Version 5.41 (November 2019). Accessed April 4, 2020.
(29) Martin, D.; Moraleda, D.; Achard, T.; Giordano, L.; Buono, G. Assessment of the electronic properties of p ligands stemming from secondary phosphine oxides. *Chem. − Eur. J.* **2011**, *17*, 12729−12740.
(30) Fairlamb, I. J. S.; Grant, S.; Whitwood, A. C.; Whitthall, J.; Batsanov, A. S.; Collings, J. C. Synthesis of Pd(II) and Pt(II) complexes possessing bicyclo[3.2.0]heptanyl phosphinite ligands: Identification of a novel Pd(II) precatalyst for 1,6-diene cycloisomerisation. *J. Organomet. Chem.* **2005**, *690*, 4462−4477.
(31) (a) Proutiere, F.; Schoenebeck, F. Solvent effect on palladium-catalyzed cross-coupling reactions and implications on the active catalytic species. *Angew. Chem., Int. Ed.* **2011**, *50*, 8192−8195. (b) Proutiere, F.; Schoenebeck, F. Orthogonal selectivities under Pd(0) catalysis with solvent polarity: an interplay of computational and experimental studies. *Synlett* **2012**, *23*, 645−648.
(32) Schoenebeck, F.; Houk, K. N. Ligand-controlled regioselectivity in palladium-catalyzed cross coupling reactions. *J. Am. Chem. Soc.* **2010**, *132*, 2496−2497.
(33) Kama, D. V.; Brink, A.; Visser, H. G. Crystal structure of bis(μ2-chlorido)-bis(di-p-tolylhydroxyphosphine-κP)-bis(di-p-tolylphosphite-κP)dipalladium(II), C56H58Cl2O4P4Pd2. *Z. Krist.-New Cryst. St.* **2016**, *231*, 1081−1083.
(34) Yang, D. X.; Colletti, S. L.; Wu, K.; Song, M.; Li, G. Y.; Shen, H. C. Palladium-catalyzed Suzuki−Miyaura coupling of pyridyl-2-boronic esters with aryl halides using highly active and air-stable phosphine chloride and oxide ligands. *Org. Lett.* **2009**, *11*, 381−384.
(35) Lu, T.; Chen, Q. Interaction Region Indicator: A simple real space function clearly revealing both chemical bonds and weak interactions. *Chem. Methods* **2021**, *1*, 231−239.
(36) Moreno-Mañas, M.; Pérez, M.; Pleixats, R. Palladium-catalyzed Suzuki-yype self-coupling of aarylboronic aacids. A mechanistic study. *J. Org. Chem.* **1996**, *61*, 2346−2351.
(37) (a) Kuninobu, Y.; Yoshida, T.; Takai, K. Palladium-catalyzed synthesis of dibenzophosphole oxides via intramolecular dehydrogenative cyclization. *J. Org. Chem.* **2011**, *76*, 7370−7376. (b) Feng, C.-G.; Ye, M.; Xiao, K.-J.; Li, S.; Yu, J.-Q. Pd(II)-catalyzed phosphorylation of aryl C−H bonds. *J. Am. Chem. Soc.* **2013**, *135*, 9322−9325. (c) Chen, T.-H.; Reddy, D. M.; Lee, C.-F. A palladium-catalyzed oxidative cross-coupling reaction between aryl pinacol boronates and H-phosphonates in ethanol. *RSC Adv.* **2017**, *7*, 30214−30220.
(38) Barder, T. E.; Walker, S. D.; Martinelli, J. R.; Buchwald, S. L. Catalysts for Suzuki−Miyaura coupling processes: Scope and studies of the effect of ligand structure. *J. Am. Chem. Soc.* **2005**, *127*, 4685−4696.
(39) (a) Lennox, A. J. J.; Lloyd-Jones, G. C. Transmetalation in the Suzuki-Miyaura coupling: the fork in the trail. *Angew. Chem., Int. Ed.* **2013**, *52*, 7362−7370. (b) Yang, C.; Zhang, L.; Lu, C.; Zhou, S.; Li, X.; Li, Y.; Yang, Y.; Li, Y.; Liu, Z.; Yang, J.; Houk, K. N.; Mo, F.; Guo, X. Unveiling the full reaction path of the Suzuki−Miyaura cross-coupling in a single-molecule junction. *Nat. Nanotechnol.* **2021**, *16*, 1214−1223.
(40) Cook, X. A. F.; de Gombert, A.; McKnight, J.; Pantaine, L. R. E.; Willis, M. C. The 2-pyridyl problem: Challenging nucleophiles in cross-coupling arylations. *Angew. Chem., Int. Ed.* **2021**, *60*, 11068−11091.
(41) Thota, R.; Lesage, D.; Gimbert, Y.; Giordano, L.; Humbel, S.; Milet, A.; Buono, G.; Tabet, J.-C. Gas-phase study of phenylacetylene and norbornadiene on a palladium(II) phosphinous acid complex: Importance of the order of introduction of the organic partners. *Organometallics* **2009**, *28*, 2735−2743.
(42) McFarlane, J.; Henderson, B.; Donnecke, S.; McIndoe, J. S. An information-rich graphical representation of catalytic cycles. *Organometallics* **2019**, *38*, 4051−4053.
(43) The Catalytic Cycle Generator: https://www.catacycle.com/

https://doi.org/10.1021/acsomega.1c06430
ACS Omega 2021, 6, 35134−35143